Nonlinear Convective Flow of Power-law Fluid over an Inclined Plate with Double Dispersion Effects and Convective Thermal Boundary Condition

P. Naveen, Ch. RamReddy, and D. Srinivasacharya

Abstract This study explores the impact of double dispersion effects on the nonlinear convective flow of power-law fluid along an inclined plate. Besides, the density differences with concentration and temperature are assumed to be larger and also convective thermal condition is considered at the boundary. Governing nonlinear partial differential equations are solved numerically using the successive linearization method (SLM) together with the local non-similarity technique. Accuracy and convergence of obtained results of successive linearization method are confirmed through error analysis. Also, present results are validated with previously published works in a special case. The present study enables us to discuss the influence of pertinent governing parameters on the heat and mass transfer rates of the fluid flow at the wall. This kind of investigation is useful in the mechanism of combustion, aerosol technology, high-temperature polymeric mixtures and solar collectors, which operate at moderate to very high temperatures and concentrations.

Keywords Power-law fluid · Nonlinear Boussinesq approximation · Convective boundary condition · Successive linearization method · Double dispersion effects

1 Introduction

Analysis of heat and mass transfer of non-Newtonian power-law fluid (Ostwald-de Waele type) flow through porous media acquired huge attention by many researchers [1–7] due its comprehensive applications in energy and geophysical industries. In the fields of oil reservoir, ceramic processing and heat storage beds, the double dispersion effects are more predominant with the consideration of inertial effects

P. Naveen (✉)
Department of Mathematics, School of Advanced Sciences, Vellore Institute of Technology, Vellore 632014, India
e-mail: naveen.p@vit.ac.in

Ch. RamReddy · D. Srinivasacharya
Department of Mathematics, National Institute of Technology Warangal, Warangal 506004, India

S. S. Ray et al. (eds.), *Applied Analysis, Computation and Mathematical Modelling in Engineering*, Lecture Notes in Electrical Engineering 897,
https://doi.org/10.1007/978-981-19-1824-7_8

in the flow region of porous medium (refer Nield and Bejan [8]). Moreover, the fluid flow through intricate paths activates dispersion effects in porous media at pore level. With this consideration, the importance of the thermal and solutal dispersion on the flow of fluid through a porous medium are exhibited by many authors. A lot of research has been accounted-for on this point with different fluids as depicted in the articles of researchers [9–13].

In addition to the above said point, double dispersion effects are more prevalent in fluid flow regime when the temperature–concentration-dependent density relation is nonlinear (also known as, nonlinear Boussinesq approximation [14, 15]) in the buoyancy term. Since, most of the thermal equipment works at moderate and very high temperatures and concentrations, this leads to have nonlinearity in buoyancy with temperature–concentration-dependent density relation [16, 17].

Heat transfer analysis with the convective thermal boundary condition is beneficial consideration and has very important applications in the of fields nuclear plants, gas turbines, heat exchangers related industries. In view of these applications, Munir [18] (on viscous fluid flow), Hayat [19] (on power-law fluid flow) and RamReddy and Naveen [20] (on micropolar fluid flow) considered this thermal condition at the boundary for the study of fluid flow behaviour over different geometries.

In the present study, the heat and mass transport phenomena of power-law fluid past an inclined plate with a convective thermal boundary condition is examined. The double dispersion effects and nonlinear Boussinesq approximations are included in order to investigate their effect over fluid flow.

2 Governing Equations

Consider, the steady, 2D, laminar mixed convective flow of incompressible power-law fluid along an inclined plate in a non-Darcy porous medium. The inclination angle is measured in terms of Ω about vertical direction. By left convection, the infinite plate is either heated or cooled from a fluid with temperature T_f. The solutal concentration over the wall is C_w, and ambient porous medium concentration and temperature are taken to be C_∞ and T_∞, respectively.

By employing nonlinear Boussinesq approximation and with usual boundary layer conditions, the governing equations for the power-law fluid flow in a non-Darcy porous medium (Forchheimer model) [2, 21, 22] are given by

$$\frac{\partial u}{\partial x} + \frac{\partial v}{\partial y} = 0 \tag{1}$$

$$\frac{\partial u^n}{\partial y} + \frac{b\sqrt{K_p}}{\nu}\frac{\partial u^2}{\partial y} = \frac{K_p g^*}{\nu}\left\{[\beta_0 + 2\beta_1(T - T_\infty)]\frac{\partial T}{\partial y} + [\beta_2 + 2\beta_3(C - C_\infty)]\frac{\partial C}{\partial y}\right\}\cos\Omega \tag{2}$$

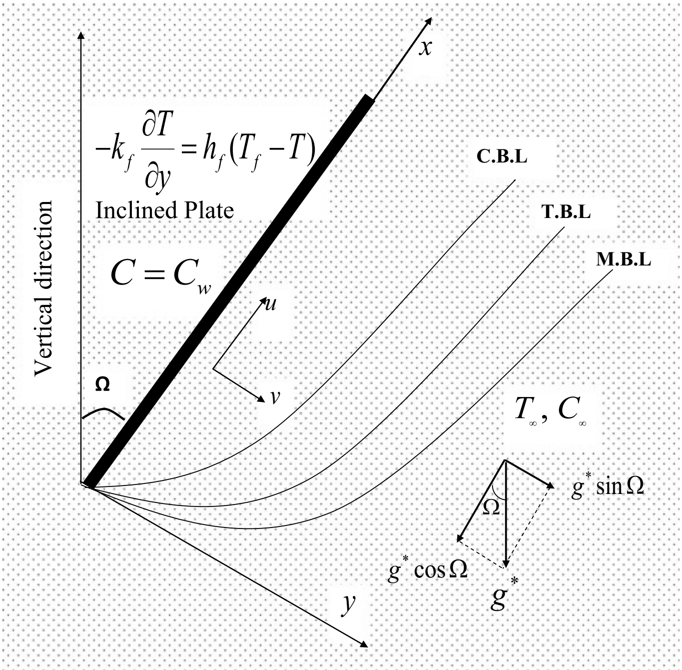

Fig. 1 Schematic diagram of the problem

$$u\frac{\partial T}{\partial x} + v\frac{\partial T}{\partial y} = \frac{\partial}{\partial y}\left[(\alpha + \chi\, d\, u)\frac{\partial T}{\partial y}\right] \tag{3}$$

$$u\frac{\partial C}{\partial x} + v\frac{\partial C}{\partial y} = \frac{\partial}{\partial y}\left[(D + \zeta\, d\, u)\frac{\partial C}{\partial y}\right] \tag{4}$$

The associated boundary conditions are

$$\begin{gathered} v = 0,\quad -k_f\frac{\partial T}{\partial y} = h_f(T_f - T),\quad C = C_w \quad \text{at} \quad y = 0 \\ u = u_\infty,\quad T = T_\infty,\quad C = C_\infty \quad \text{as} \quad y \to \infty \end{gathered} \tag{5}$$

where u and v are the velocity components in x and y directions, T is the temperature, C is the concentration, b is the empirical constant associated with the Forchheimer porous inertia term, n is the power-law index, Ω is the inclination angle, g^* is the acceleration due to gravity, K_p is the permeability, ν is the kinematic viscosity, k_f is the thermal conductivity of the fluid, h_f is the convective heat transfer coefficient, α is the molecular thermal diffusivity, D is the molecular solutal diffusivity, d is the pore diameter, χ is the thermal dispersion coefficient and ζ is the solutal dispersion coefficient, respectively.

Further, the first- and second-order expansions of thermal coefficients are denoted by β_0 and β_1. Like that, the first- and second-order expansions of solutal coefficients are defined by β_2 and β_3, respectively.

Now introduce stream function $\psi(x, y)$ as $u = \dfrac{\partial \psi}{\partial y}$ and $v = -\dfrac{\partial \psi}{\partial x}$, which is automatically satisfied the continuity equation (1).

Here, we define non-similarity transformations [23–25] in the following form

$$
\begin{gathered}
\xi = \frac{x}{L}, \quad Pe = \frac{u_\infty L}{\alpha}, \eta = \frac{y}{L} Pe^{\frac{1}{2}} \xi^{\frac{-1}{2}}, \quad \psi(\xi, \eta) = \alpha \xi^{\frac{1}{2}} Pe^{\frac{1}{2}} f(\xi, \eta) \\
T(\xi, \eta) = T_\infty + \left(T_f - T_\infty\right) \theta(\xi, \eta), \quad C(\xi, \eta) = C_\infty + (C_w - C_\infty) \phi(\xi, \eta)
\end{gathered} \tag{6}
$$

where ξ is the stream-wise coordinate, L is the characteristics length and $Pe = \frac{u_\infty L}{\alpha}$ is the global Peclet's number. f, θ and ϕ are the dimensionless stream function, temperature and concentrations, respectively.

Substituting the transformations (6) into (1)–(4), we obtain the non-dimensional governing equations,

$$
n \left(f'\right)^{n-1} f'' + 2F_0 Pe f' f'' = \lambda^n \left[(1 + 2\alpha_1\theta)\theta' + \mathcal{B}(1 + 2\alpha_2\phi)\phi'\right] \cos\Omega \tag{7}
$$

$$
\theta'' + Pe_\chi \left(f' \theta'\right)' + \frac{1}{2} f \theta' = \xi \left(f' \frac{\partial \theta}{\partial \xi} - \frac{\partial f}{\partial \xi} \theta'\right) \tag{8}
$$

$$
\frac{1}{Le} \phi'' + Pe_\zeta \left(f' \phi'\right)' + \frac{1}{2} f \phi' = \xi \left(f' \frac{\partial \phi}{\partial \xi} - \frac{\partial f}{\partial \xi} \phi'\right) \tag{9}
$$

The resultant boundary conditions from Eq. (5)

$$
\begin{gathered}
f(\xi, 0) = -2\xi \left(\frac{\partial f}{\partial \xi}\right)_{\eta=0}, \quad \theta'(\xi, 0) = -Bi\, \xi^{\frac{1}{2}} \left[1 - \theta(\xi, 0)\right], \phi(\xi, 0) = 1, \\
f'(\xi, \infty) = 1, \ \theta(\xi, \infty) = 0, \ \phi(\xi, \infty) = 0.
\end{gathered} \tag{10}
$$

In the above equations, Ra denotes the global Rayleigh number, λ denotes the mixed convection parameter, $F_0 Pe$ denotes the Forchheimer number, $\mathcal{B}$ denotes the and Buoyancy ratio, Ω denotes the angle of inclination, Pe_d denotes the pore diameter-dependent Péclet number, Pe_χ denotes the thermal dispersion parameter, Le denotes the diffusivity ratio, Pe_ζ denotes the solutal dispersion parameter, α_1 denotes the nonlinear density–temperature parameter (NDT), Bi denotes the Biot number, and α_2 denotes the nonlinear density–concentration parameter (NDC).

Mathematical expressions for the parameters are given below, $Ra = (\frac{L}{\alpha}) \left(\frac{[K_p g^* \beta_0 (T_f - T_\infty)]}{\nu}\right)^{1/n}, \lambda = \frac{Ra}{Pe}, F_0 Pe = f_0 (Pe_d)^{2-n} \left(f_0 = \left[\frac{(b\sqrt{K_p})}{\nu}\right] (\frac{\alpha}{d})^{2-n}\right), \mathcal{B} =$

$\frac{\beta_2(C_w-C_\infty)}{(\beta_0(T_f-T_\infty))}$, $Pe_d = \frac{(u_\infty d)}{\alpha}$, $Pe_\chi = \frac{[\chi\, d\, u_\infty]}{\alpha}$, $Le = \frac{\alpha}{D}$, $Pe_\zeta = \frac{[\zeta\, d\, u_\infty]}{\alpha}$, $\alpha_1 = \frac{\beta_1(T_f-T_\infty)}{\beta_0}$, $\alpha_2 = \frac{\beta_3(C_w-C_\infty)}{\beta_2}$ and $Bi = \frac{h_f L}{(k_f\ Pe^{1/2})}$.

Here, the physical quantities of interest, the non-dimensional Nusselt and the Sherwood numbers are given by

$$Nu Pe^{\frac{-1}{2}} = -\xi^{\frac{1}{2}}\left[1 + Pe_\chi\, f'(\xi, 0)\right]\theta'(\xi, 0),\ \ Sh Pe^{\frac{-1}{2}} = -\xi^{\frac{1}{2}}\left[1 + Pe_\zeta\, f'(\xi, 0)\right]\phi'(\xi, 0).$$

3 Numerical Solution

For the solutions of partial differential equations (7)–(9) together with (10), the following steps were followed

- Firstly, the above-said PDEq equations are transformed into ODEqs [26] by introducing auxiliary variables.
- Next, a novel successive linearization method is used to linearize the resultant equations.
- Lastly, the linearized equations are solved with the Chebyshev collocation method [27–29].

The detailed procedure of solution methodology to solve equations (7)–(9) together with (10) is presented in the following Sects. 3.1 to 3.3.

3.1 Local Non-similarity Procedure

The preliminary approximate solution can be found from local similarity equations for a particular case of $\xi << 1$; the terms containing $\xi \frac{\partial}{\partial \xi}$ are supposed to be negligible. Then, the first-level truncation or local similarity equations from (7)–(10) are

$$\left[n\left(f'\right)^{n-1} + 2F_0 Pe f'\right]f'' - \lambda^n\left[(1+2\alpha_1\theta)\theta' + \mathcal{B}(1+2\alpha_2\phi)\phi'\right]\cos\Omega = 0 \tag{11}$$

$$\theta'' + Pe_\chi\left(f'\theta'\right)' + \frac{1}{2}f\theta' = 0 \tag{12}$$

$$\frac{1}{Le}\phi'' + Pe_\zeta\left(f'\phi'\right)' + \frac{1}{2}f\phi' = 0 \tag{13}$$

The corresponding boundary conditions are

$$\begin{aligned} f(\xi,0)=0,\ \theta'(\xi,0)=-Bi\,\xi^{\frac{1}{2}}\left[1-\theta(\xi,0)\right],\phi(\xi,0)=1,\\ f'(\xi,\infty)=1,\ \theta(\xi,\infty)=0,\ \phi(\xi,\infty)=0. \end{aligned} \tag{14}$$

The local non-similarity ordinary nonlinear differential equations in the second-level truncation is discovered by introducing new variables to recall the omitted expressions from the first-level truncation, i.e. take $U=\dfrac{\partial f}{\partial \xi}$, $V=\dfrac{\partial \theta}{\partial \xi}$, $W=\dfrac{\partial \phi}{\partial \xi}$. Thus, the second-level truncation is

$$\left[n\,\left(f'\right)^{n-1}+2F_0Pef'\right]f''-\lambda^n\left[(1+2\,\alpha_1\theta)\theta'+\mathcal{B}(1+2\,\alpha_2\phi)\phi'\right]\cos\Omega=0 \tag{15}$$

$$\theta''+\ Pe_\chi\left(f'\,\theta'\right)'+\frac{1}{2}f\theta'=\xi\left(V\,f'-U\,\theta'\right) \tag{16}$$

$$\frac{1}{Le}\phi''+\ Pe_\zeta\left(f'\,\phi'\right)'+\frac{1}{2}f\phi'=\xi\left(W\,f'-U\,\phi'\right) \tag{17}$$

The corresponding boundary conditions are

$$\begin{aligned} f(\xi,0)=-2\,\xi\,U(\xi,\eta),\ \theta'\,(\xi,0)=-Bi\,\xi^{\frac{1}{2}}\left[1-\theta(\xi,0)\right],\ \phi(\xi,0)=1,\\ f'(\xi,\infty)=1,\ \theta(\xi,\infty)=0,\ \phi(\xi,\infty)=0. \end{aligned} \tag{18}$$

The two-level local non-similarity technique is accomplished with a third level of truncation; for this, we differentiate equations (15)–(18) with respect to ξ and omit the partial derivatives of U, V, W. Then, the resultant equations are

$$\begin{aligned} n(n-1)\left(f'\right)^{n-2}f''U'+n\left(f'\right)^{n-1}U''+2F_0Pe(f''U'+U''f')-\\ \lambda^n\left[V'+2\,\alpha_1(V\theta'+\theta V')+\mathcal{B}(W'+2\,\alpha_2(W\phi'+\phi W'))\right]\cos\Omega=0 \end{aligned} \tag{19}$$

$$V''+\frac{3}{2}U\theta'+\frac{1}{2}V'f+Pe_\chi\left[U''\,\theta'+f''\,V'+U'\,\theta''+f'\,V''\right]-V\,f'=\xi\left(U'V-UV'\right) \tag{20}$$

$$\frac{1}{Le}W''+\frac{3}{2}U\phi'+\frac{1}{2}W'f+Pe_\zeta\left[U''\,\phi'+f''\,W'+U'\,\phi''+f'\,W''\right]-Wf'=\xi\left(U'W-UW'\right) \tag{21}$$

The corresponding boundary conditions are

$$\begin{aligned} U(\xi,0)=0,\,V'\,(\xi,0)=Bi\xi^{\frac{1}{2}}V\,(\xi,0)+\frac{1}{2}Bi\xi^{\frac{-1}{2}}[\theta(\xi,0)-1],\,W(\xi,0)=0,\\ U'(\xi,\infty)=0,\,V\,(\xi,\infty)=0,\,W(\xi,\infty)=0 \end{aligned} \tag{22}$$

The coupled nonlinear ordinary differential equations (15)–(17) and (19)–(21) along with the boundary conditions (18) and (22) are evaluated using successive linearization method. First, it linearize the non-similarity equation, and then, it utilizes Chebyshev collocation method for the approximate solution.

3.2 Successive Linearization

Let us consider an independent vector $\mathbb{Q}(\eta) = [f(\eta), \theta(\eta), \phi(\eta), U(\eta), V(\eta), W(\eta)]$ and assume that it can be represented as

$$\mathbb{Q}(\eta) = \mathbb{Q}_k(\eta) + \sum_{m=0}^{k-1} \mathbb{Q}_m(\eta) \tag{23}$$

where $\mathbb{Q}_k(\eta),\ k = 1, 2, 3\ldots$ are unknown vectors, and those are determined by recursively evaluating the linearized version of the non-similarity equations and presuming that $\mathbb{Q}_m(\eta),\ (0 \leq m \leq k-1)$ are expected from antecedent iterations. The initial guesses $\mathbb{Q}_0(\eta)$ is selected so that it satisfy the boundary conditions (18) and (22). By imposing Eq. (23) in Eqs.(15)–(22) and considering only linear terms, we obtain the linearized equations to be evaluated which are

$$\tilde{p}_{1,k-1} f_k'' + \tilde{p}_{2,k-1} f_k' + \tilde{p}_{3,k-1}\theta_k' + \tilde{p}_{4,k-1}\theta_k + \tilde{p}_{5,k-1}\phi_k' + \tilde{p}_{6,k-1}\phi_k = \tilde{z}_{1,k-1} \tag{24}$$

$$\tilde{q}_{1,k-1} f_k + \tilde{q}_{2,k-1}\theta_k'' + \tilde{q}_{3,k-1}\theta_k' + \tilde{q}_{4,k-1} U_k + \tilde{q}_{5,k-1} V_k = \tilde{z}_{2,k-1} \tag{25}$$

$$\tilde{a}_{1,k-1} f_k + \tilde{a}_{2,k-1}\phi_k'' + \tilde{a}_{3,k-1}\phi_k' + \tilde{a}_{4,k-1} U_k + \tilde{a}_{5,k-1} W_k = \tilde{z}_{3,k-1} \tag{26}$$

$$\begin{aligned}\tilde{b}_{1,k-1} f_k'' + \tilde{b}_{2,k-1} f_k' + \tilde{b}_{3,k-1}\theta_k' + \tilde{b}_{4,k-1}\theta_k + \tilde{b}_{5,k-1}\phi_k' + \tilde{b}_{6,k-1}\phi_k + \tilde{b}_{7,k-1} U_k'' + \tilde{b}_{8,k-1} U_k' \\ + \tilde{b}_{9,k-1} V_k' + \tilde{b}_{10,k-1} V_k + \tilde{b}_{11,k-1} W_k' + \tilde{b}_{12,k-1} W_k = \tilde{z}_{4,k-1}\end{aligned} \tag{27}$$

$$\tilde{c}_{1,k-1} f_k + \tilde{c}_{2,k-1}\theta_k' + \tilde{c}_{3,k-1} U_k' + \tilde{c}_{4,k-1} U_k + \tilde{c}_{5,k-1} V_k'' + \tilde{c}_{6,k-1} H_k' + \tilde{c}_{7,k-1} V_k = \tilde{z}_{5,k-1} \tag{28}$$

$$\tilde{d}_{1,k-1} f_k + \tilde{d}_{2,k-1}\phi_k' + \tilde{d}_{3,k-1} U_k' + \tilde{d}_{4,k-1} U_k + \tilde{d}_{5,k-1} W_k'' + \tilde{d}_{6,k-1} W_k' + \tilde{d}_{7,k-1} W_k = \tilde{z}_{6,k-1} \tag{29}$$

The linearised boundary conditions are

$$\begin{aligned} f_k(0) = f_k'(0) = f_k'(\infty) = 0,\ Bi\,\xi^{\frac{1}{2}}\theta_k(0) + \theta_k'(0) = 0,\ \theta_k(\infty) = 0, \\ \phi_k(0) = \phi_k(\infty) = 0,\ U_k(0) = U_k'(0) = U_k'(\infty) = 0, \\ -\frac{1}{2} Bi\,\xi^{\frac{-1}{2}}\theta_k(0) + V_k'(0) - Bi\,\xi^{\frac{1}{2}} V_k(0) = 0,\ V_k(\infty) = 0,\ W_k(0) = W_k(\infty) = 0 \end{aligned} \tag{30}$$

Here, the coefficient parameters $\tilde{p}_{s,k-1}$, $\tilde{q}_{s,k-1}$, $\tilde{a}_{s,k-1}$, $\tilde{b}_{s,k-1}$, $\tilde{c}_{s,k-1,}$ $\tilde{d}_{s,k-1}$, and $\tilde{z}_{s,k-1}$ which depend on the $\mathbb{Q}_0(\eta)$ and on the $\mathbb{Q}_k(\eta)$ derivatives.

3.3 Chebyshev Collocation Scheme

We solve linearized equations (24)–(29) by an established procedure, namely Chebyshev collocation scheme [30]. In the context of numerical implication, the original region $[0, \infty)$ is truncated to $[0, L]$ for large value of L, and further, the truncated region $[0, L]$ is transformed into $[-1, 1]$ using the following mapping

$$\frac{\eta}{L} = \frac{\tau + 1}{2}, \qquad -1 \le \tau \le 1 \tag{31}$$

In this procedure, The Chebyshev polynomials $T_m(\tau) = \cos[m \ \cos^{-1}\tau]$ are used to approximate the unknown functions $\mathbb{Q}_k(\eta)$ and these polynomials are collocated at $K + 1$ Gauss–Lobatto points in the interval $[-1, 1]$ and those are defined as

$$\tau_m = \cos\frac{\pi m}{K}, \qquad m = 0, 1, ..., K \tag{32}$$

The unknown function $\mathbb{Q}_k(\eta)$ is imprecise at the collocation points by

$$\mathbb{Q}_k(\tau) = \sum_{j=0}^{K} \mathbb{Q}_k(\tau_j) T_j(\tau_m), \qquad m = 0, 1, ...K \tag{33}$$

and

$$\frac{d^{\mathbb{S}}}{d\eta^{\mathbb{S}}}\mathbb{Q}_k(\tau) = \sum_{r=0}^{K} \mathbf{D}^{\mathbb{S}}_{rm}\mathbb{Q}_k(\tau_r), \qquad m = 0, 1, 2, ...K \tag{34}$$

where $\mathcal{D}$ is the Chebyshev spectral derivative matrix such that $\mathbf{D} = (2/L)\mathcal{D}$ and $\mathbb{S}$ is the order of differentiation. After employing Eqs.(31)–(34) into linearized form of Eqs. (24)–(29), the resultant solution is

$$\tilde{\mathbf{Y}}_k = \tilde{\mathbf{B}}^{-1}_{k-1}\tilde{\mathbf{Z}}_{k-1} \tag{35}$$

In Eq. (35), $\tilde{\mathbf{B}}_{k-1}$ is a $(6N + 6) \times (6N + 6)$ matrix, $\tilde{\mathbf{Y}}_k$ and $\tilde{\mathbf{Z}}_{k-1}$ are $(6N + 1) \times 1$ column vectors defined by

$$\begin{aligned} \tilde{\mathbf{B}}_{k-1} = \left[\tilde{\mathbf{B}}_{ij}\right],\ i, j = 1, 2, \ldots 6,\ \ \tilde{\mathbf{Y}}_k = \left[\tilde{\mathbb{F}}_k\ \tilde{\Theta}_k\ \tilde{\Phi}_k\ \tilde{\mathbb{U}}_k\ \tilde{\mathbb{V}}_k\ \tilde{\mathbb{W}}_k\right]^T, \\ \tilde{\mathbf{Z}}_{k-1} = \left[\tilde{\mathbf{z}}_{1,k-1}\ \tilde{\mathbf{z}}_{2,k-1}\ \tilde{\mathbf{z}}_{3,k-1}\ \tilde{\mathbf{z}}_{4,k-1}\ \tilde{\mathbf{z}}_{5,k-1}\ \tilde{\mathbf{z}}_{6,k-1}\right]^T \end{aligned} \tag{36}$$

3.4 Residual Error Analysis

It can be ensured the convergence of the proposed method by evaluating the norm of the difference between two consecutive iterations. This algorithm is accepted to have converged when the error norms are less than a given tolerance level. The error norms are given by

$$E_f = \max_{0\le i\le Nx} \parallel f_{r+1,i} - f_{r,i} \parallel_\infty, E_\theta = \max_{0\le i\le Nx} \parallel \theta_{r+1,i} - \theta_{r,i} \parallel_\infty, \\ E_\phi = \max_{0\le i\le Nx} \parallel \phi_{r+1,i} - \phi_{r,i} \parallel_\infty \tag{37}$$

Norm of the residual errors of the governing Eqs. (7)–(9) across ξ at different iterations levels of the present numerical scheme are depicted by Fig. 2. This figure revels that the residual errors decrease with an increase of number of iterations, and this is an indication of convergence of the solutions. Also, observed that the residual errors are nearly uniform across ξ. This result proves that the accuracy of solution method does not depend on the length of ξ interval. Furthermore, the small residual errors, which are obtained after a few iterations, are a clear sign of the accuracy of the solution method. Hence, the residual error results validate the accuracy of generated results in this study.

4 Results and Discussion

In addition to the error analysis, present numerical results are also validated with the previously published works [9, 31] without nonlinear convection and double dispersion effects as appeared in Tables 1 and 2. Results are in good agreement, and the influence of the parameters α_1, α_2, Pe_χ, Pe_ζ, Ω and Bi are depicted by the Figs. 3, 4 and 5 for f', θ, ϕ, $Nu\,Pe^{\frac{-1}{2}}$ and $Sh\,Pe^{\frac{-1}{2}}$.

4.1 Influence of α_1 and α_2 With Viscosity Index n

Variations of fluid flow profiles for $\alpha_1(0, 6)$, α_2 $(0, 5)$ and n (0.7, 1.0, 1.4) with $Pe_\chi = 0.5$, $Pe_\zeta = 0.2$, $Bi = 0.5$, $\xi = 0.5$ and $\Omega = 30°$ shown in Fig. 3a–c. It uncovers that the influence of n is extensive and increases both thermal and solutal boundary layer thickness, whereas it diminishes the thickness of momentum boundary layer. Regarding α_1, the velocity is predominant at the inclined plate surface and for η_{max} value, it achieves unity. As found in Fig. 3a, $\alpha_1 > 0$ infers that $T_f > T_\infty$; henceforth, some amount of the heat is induced to fluid region by the wall surface. Moreover, Fig. 3a displays the impact of the α_2 on the behaviour of velocity. The results of this figure repeat the same kind of behaviour just like α_1 in all three fluids. The thicknesses of thermal and solutal boundary layer diminish with the rise of both α_1

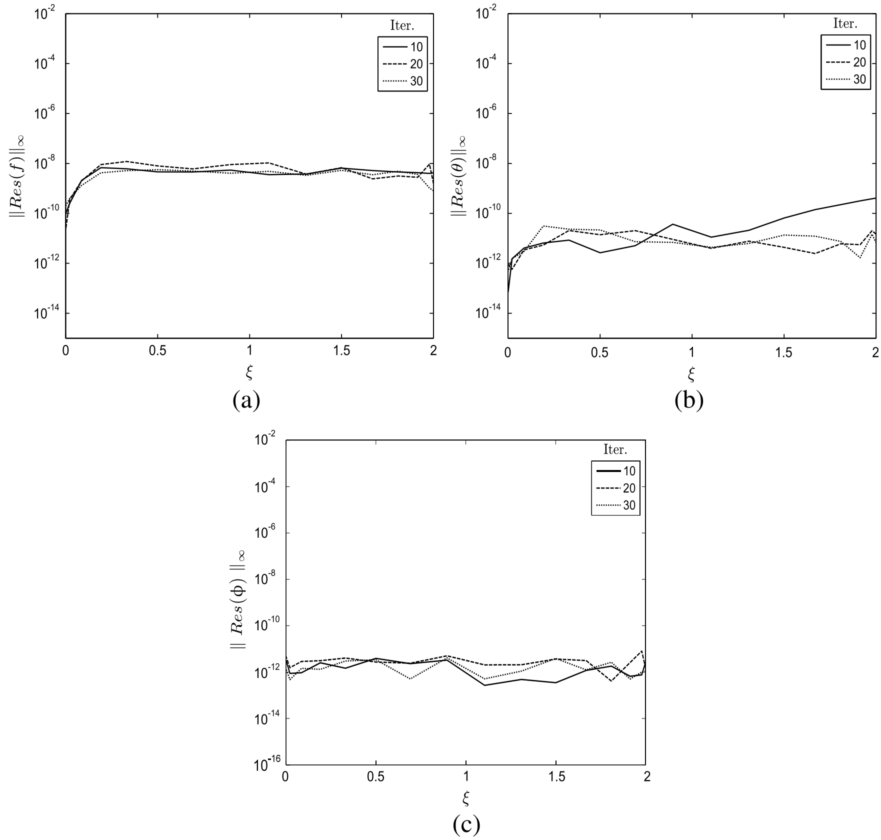

Fig. 2 Residual error over iterations when $\mathcal{B} = 0.5$, $F_0 Pe = 1, \alpha_1 = 1, \alpha_2 = 1$, $Bi = 0.5, n = 1$, $Pe_\chi = 0.5$, $Pe_\zeta = 0.2$, $\Omega = 30°$

and α_2, as shown in Fig. 3b, c. Obviously, the nonlinear temperature and concentration differences between the wall and ambient medium are increased for larger values of α_1 and α_2, due to which higher velocity and smaller temperature concentration are obtained.

Figure 3d–e show the effect of $\alpha_1(0, 6)$ and $\alpha_2(0, 5)$ on the $NuPe^{-1/2}$ and $ShPe^{-1/2}$ against ξ. The rise of either α_1 or α_2 increases all the fluid profiles of the pseudo-plastic fluid flow. So, also, these two dimensionless quantities have a same change in the other two fluid flows of Newtonian and dilatant fluid. Evidently, these two heat and mass transfer rates are identically comparable with the works of Partha [16] in Newtonian fluid (for $n = 1$) case.

Table 1 Comparison of $-\theta'(0)$ against λ with the fixed values of $\mathcal{B}=0$, $F_0 Pe=0$, $\alpha_1=0$, $Bi\to\infty$, $\alpha_2=0$, $Pe_\chi=0$, $Pe_\zeta=0$ and $\Omega=0$

	$n=0.5$		$n=1.0$		$n=1.5$	
λ	[31]	Present	[31]	Present	[31]	Present
0	0.5641	0.5642	0.5641	0.5642	0.5641	0.5642
0.5	0.8209	0.8217	0.6473	0.6474	0.6034	0.6034
1.0	0.9303	0.9296	0.7205	0.7206	0.6634	0.6634
4.0	1.3010	1.3007	1.0250	1.0558	1.0180	1.0176
8.0	1.6100	1.6097	1.3540	1.3801	1.3800	1.4357
15.0	2.0010	2.0005	1.8120	1.8123	1.8620	1.8606

Table 2 Comparison of $f'(0)$, $-\theta'(0)$ and $-\phi'(0)$ against $Le, \mathcal{B}, \lambda$ with the fixed values of $F_0 Pe=1$, $n=1$, $Pe_\chi=0$, $\alpha_2=0$, $Pe_\zeta=0$, $Bi\to\infty$, $\alpha_1=0$ and $\Omega=0$

				$Le=1$		$Le=10$			
		$f'(0)$		$-\theta'(0)$ & $-\phi'(0)$		$-\theta'(0)$		$-\phi'(0)$	
	λ	[9]	Present	[9]	Present	[9]	Present	[9]	Present
$\mathcal{B}=-0.5$	0	1.0	1.0	0.5645	0.5642	0.5642	0.5642	1.7841	1.7841
	1	1.1583	1.1583	0.5922	0.5922	0.6054	0.6054	1.9329	1.9329
	5	1.6794	1.6794	0.6793	0.6793	0.7244	0.7244	2.3534	2.3534
	10	2.1926	2.1926	0.7580	0.7580	0.8247	0.8247	2.7009	2.7009
	20	3.0	3.0	0.8706	0.8706	0.9617	0.9617	3.1686	3.1686
$\mathcal{B}=1.0$	0	1.0	1.0	0.5642	0.5642	0.5642	0.5642	1.7841	1.7841
	1	1.5616	1.5616	0.6603	0.6603	0.6377	0.6377	2.1381	2.1381
	5	3.0	3.0	0.8706	0.8706	0.8083	0.8083	2.8864	2.8865
	10	4.217	4.2167	1.0203	1.0203	0.9358	0.9358	3.4061	3.4061
	20	6.0	6.0	1.2097	1.2097	1.1012	1.1012	4.0548	4.0548

4.2 *Influence of* Ω *and* Bi *With Viscosity Index* n

Effect of $\Omega(0°, 60°)$ and $Bi(0.1, 10)$ on the f', θ and ϕ are displayed in Fig. 4a–c for three instances of viscosity index ($n=0.7, 1.0, 1.4$). As depicted in Fig. 4a, reduction in the buoyancy effect caused by Ω diminishes the velocity f'. Also, it is observed from Fig. 4a that the velocity of the power-law fluid enhances by magnifying Bi. With rising values of Ω values of θ and ϕ enhance, as show in Fig. 4b, c, and these results are qualitatively matched with the work of Chen [32].

Impact of Bi on the θ is collected through Fig. 4b for the case of wall and non-isothermal conditions. Since, convective thermal condition can be changed to wall condition for a larger value of Bi (i.e. $Bi\to\infty$) [33], the same was observed from Fig. 4b. At the wall surface, the temperature is accelerating when Bi changing from $Bi<0.1$ (known as, thermally thin case) to $Bi>0.1$ (known as, thermally thick case). Further, that the concentration decreasing function of Bi, as shown in Fig. 4c.

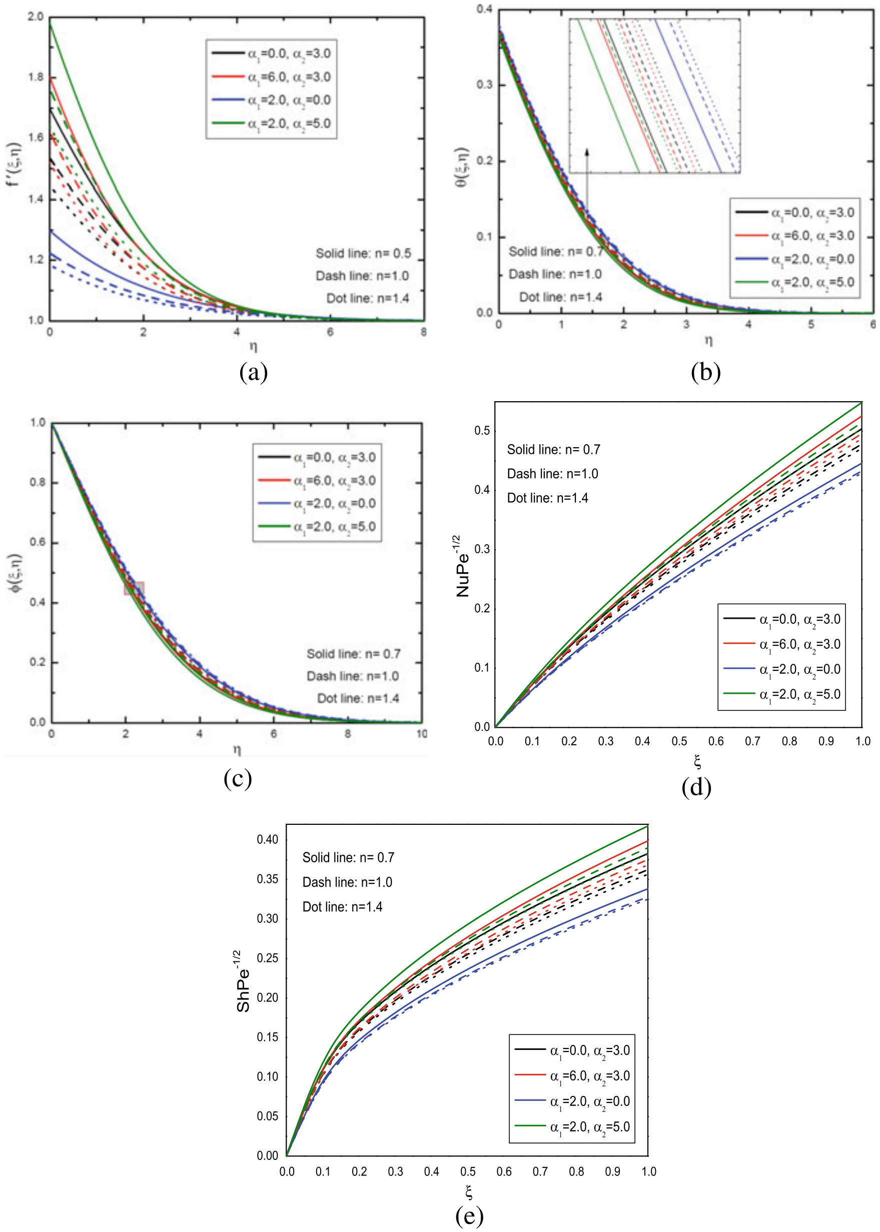

Fig. 3 Impact of α_1 and α_2 on the **(a)** f', **(b)** θ, **(c)** ϕ, **(d)** $Nu\, Pe^{\frac{-1}{2}}$, and **(e)** $Sh\, Pe^{\frac{-1}{2}}$ for three values of n with $Bi = 0.5$, $Pe_\chi = 0.5$, $Pe_\zeta = 0.2$, $\Omega = 30°$

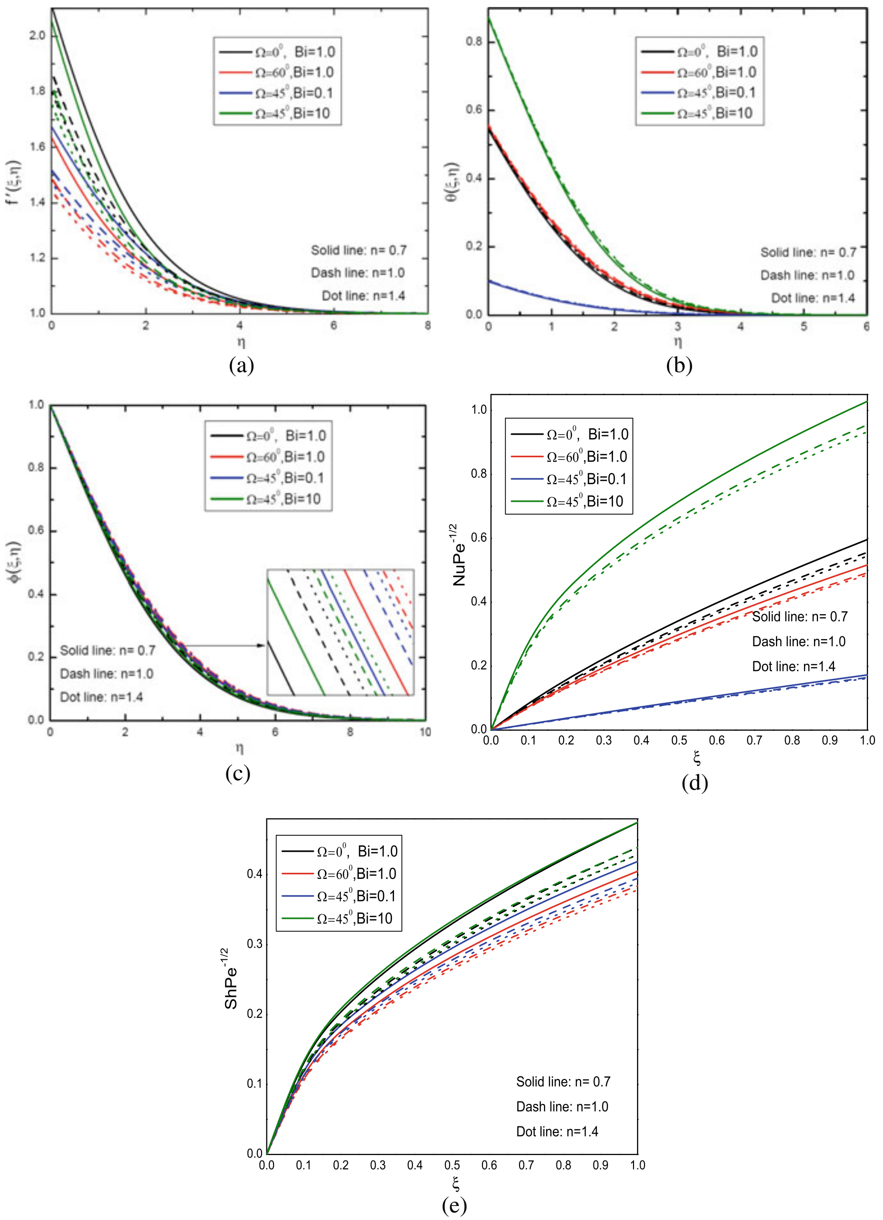

Fig. 4 Impact of Ω and Bi on the **(a)** f', **(b)** θ, **(c)** ϕ, **(d)** $Nu\,Pe^{\frac{-1}{2}}$, and **(e)** $Sh\,Pe^{\frac{-1}{2}}$ for three values of n with $\alpha_1 = 1$, $Pe_\chi = 0.5$, $\alpha_2 = 1$, $Pe_\zeta = 0.2$

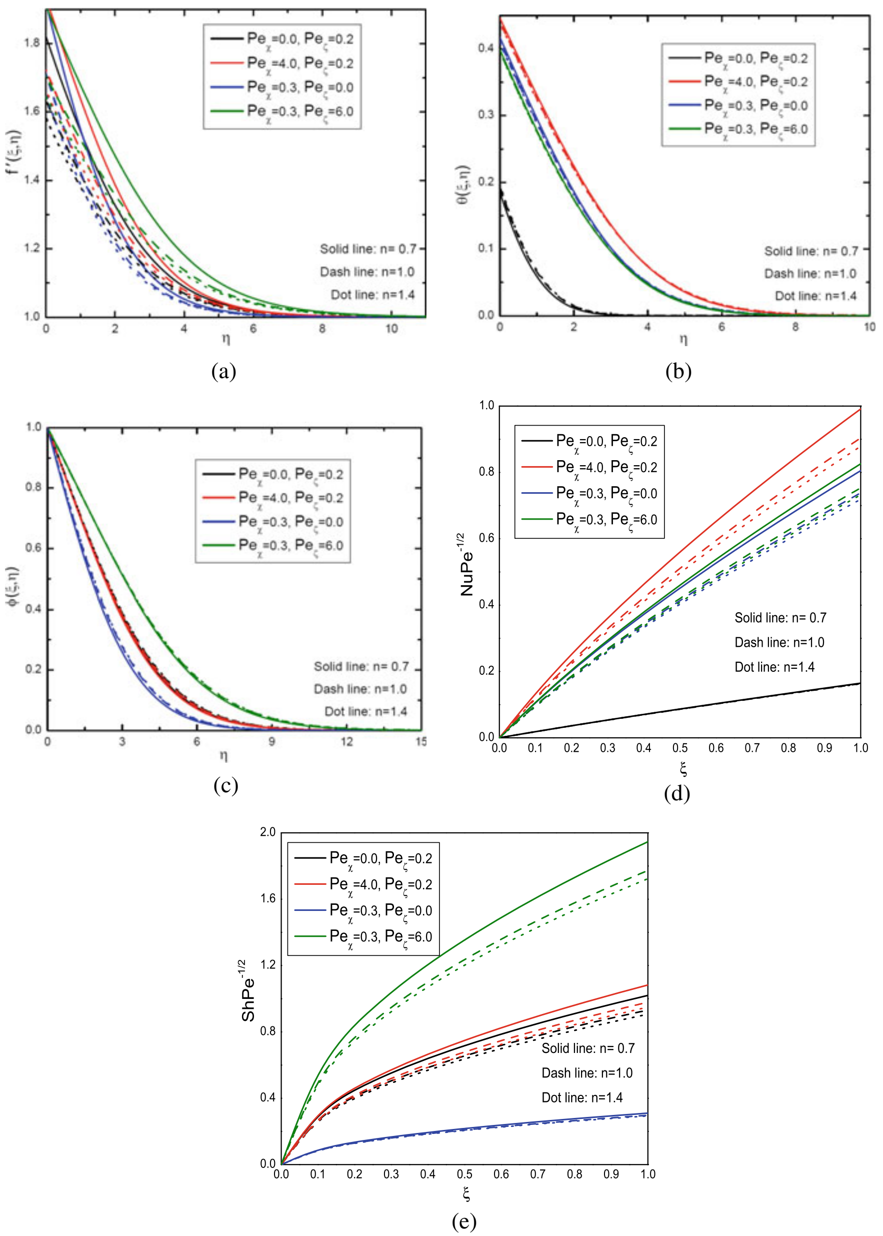

Fig. 5 Impact of Pe_χ and Pe_ζ on the **(a)** f', **(b)** θ, **(c)** ϕ, **(d)** $Nu\ Pe^{\frac{-1}{2}}$, and **(e)** $Sh\ Pe^{\frac{-1}{2}}$ for three values of n with $Bi = 0.3, \alpha_1 = 1, \alpha_2 = 1, \Omega = 30°$

Table 3 Parameters in the model and their values

Parameters	Symbol	Value range	Source
Biot number	Bi	(0, 10)	[19, 34]
Angle of inclination	Ω	$(0^0, 90^0)$	[35, 36]
NDT parameter	α_1	(0, 6)	[16]
Thermal dispersion parameter	Pe_χ	(0, 4)	[11, 13]
NDC parameter	α_2	(0, 5)	[16]
Solutal dispersion parameter	Pe_ζ	(0, 6)	[11, 13]
Power-law index	n	(0.5, 1.5)	[36]

Figure 4d–e exhibit the effect of $\Omega\,(0°, 60°)$ and $Bi\,(0.1, 10)$ on the $NuPe^{-1/2}$ and $ShPe^{-1/2}$ for three fluid cases with $Pe_\chi = 0.6$, $Pe_\zeta = 0.3, \alpha_1 = 1, \alpha_2 = 1$. If position of plate is changing from vertical to horizontal, there is a decrement in $g^* cos\Omega$ term, and this degrade the buoyancy. Hence, this reduction diminishes $NuPe^{-1/2}$ and $ShPe^{-1/2}$. However, $NuPe^{-1/2}$ and $ShPe^{-1/2}$ enhance by the increase of Bi and decrease with the viscosity index n (Table 3).

4.3 *Influence of Pe_χ and Pe_ζ Viscosity Index n*

Figure 5a–c revels the effect of Pe_χ $(0, 4)$, Pe_ζ $(0, 6)$ on f', θ and ϕ, for a fixed value of $\alpha_1 = 1, \alpha_2 = 1, Bi = 0.3, \xi = 0.5$ and $\Omega = 30°$. From Fig. 5a, it is significant that the thickness of the momentum boundary layer increases with the double dispersion parameters. Supplementing thermal dispersion effect into the energy equation gives more dominance in thermal conduction, and it improves thermal boundary layer thickness near to the surface of the inclined plate, as shown in Fig. 5b. On the other hand, increasing the solutal dispersion parameter leads to increase the thickness of concentration boundary layers, as depicted in Fig. 5c. However, in the absence or in the presence of double dispersion parameters, the temperature and concentration profiles are increased for viscosity index n.

The effect of $Pe_\chi\,(0, 4)$ and $Pe_\zeta = (0, 6)$ on Nusselt and Sherwood numbers is displayed in Fig. 5d–e. It is referred that thermal dispersion increases the heat transfer rate and solutal dispersion favours the mass transfer rate, as shown in Fig. 5d–e. However, these two transfer rates are more in pseudo-plastic fluids when compared with Newtonian and dilatant fluids.

5 Conclusions

In the present study, the characteristics power-law fluid flow along an inclined plate is studied with the consideration double dispersion effects and convective boundary condition at the wall. Influence of nonlinear convection parameters angle inclination is discussed. Major findings are listed below:

- Influence of α_2 is notable on the Nusselt and Sherwood number, when compared with the influence of α_1.
- Angle of inclination increases the thermal and solutal boundary layer thicknesses, whereas decreases the velocity, heat, and mass transfer rates of power-law fluid.
- Influence of Biot number is prominent in velocity, temperature, heat, and mass transfer rates.
- Heat transfer rate and temperatures of power-law fluid are magnified with by thermal dispersion parameter.
- Solutal dispersion parameter increases the concentration and mass transfer rates of power-law fluid.

Nomenclature

b	inertia coefficient which is taken to be a constant	(–)
Bi	Biot number	$\frac{h_f L}{k_f \ Pe^{\frac{1}{2}}}$
$\mathcal{B}$	buoyancy ratio	$\frac{\beta_2 (C_w - C_\infty)}{\beta_0 (T_f - T_\infty)}$
C	concentration	$\mathrm{kgmol/m^3}$
ϕ	dimensionless concentration	(–)
C_p	specific heat capacity	$\mathrm{J/(kg \cdot K)}$
C_w	wall concentration	$\mathrm{kgmol/m^3}$
C_∞	ambient concentration	$\mathrm{kgmol/m^3}$
D	solutal diffusivity	$\mathrm{m^2/s}$
f	dimensionless stream function	(–)
g^*	acceleration due to gravity	$\mathrm{m/s^2}$
h_f	convective heat transfer coefficient	$\mathrm{W/(m^2K)}$
k_f	thermal conductivity	$\mathrm{kg\,m/(K\,s^3)}$
K_p	permeability	$\mathrm{m^2}$
L	characteristic length	m
Le	diffusivity ratio	$\frac{\alpha}{D}$
n	power-law index	(–)
Nu_x	local Nusselt number	$\frac{-x}{(T_f - T_\infty)} \left[\frac{\partial T}{\partial y}\right]_{y=0}$
$Nu\,Pe^{\frac{-1}{2}}$	dimensionless Nusselt number	$-\xi^{\frac{1}{2}} \left[1 + Pe_\chi \ f'(\xi, 0)\right] \theta'(\xi, 0)$
Pe	global Peclet's number	$\frac{u_\infty L}{\alpha}$
Pe_d	pore diameter-dependent Peclet number	$\frac{u_\infty d}{\alpha}$
Pe_χ	Thermal dispersion parameter	$\frac{[\chi\, d\, u_\infty]}{\alpha}$
Pe_ζ	Solutal dispersion parameter	$\frac{[\zeta\, d\, u_\infty]}{\alpha}$
Pr	Prandtl number	$\frac{\nu}{\alpha}$
Ra	global Rayleigh number	$\left[\frac{L}{\alpha}\right] \left[\frac{K_p g^* \beta_0 (T_f - T_\infty)}{\nu}\right]^{1/n}$
$F_0 Pe$	Forchheimer number	$\left[\left(\frac{b\sqrt{K_p}}{\nu}\right) (\frac{\alpha}{d})^{2-n}\right] (Pe_d)^{2-n}$
Sh_x	local Sherwood number	$\frac{-x}{(C_w - C_\infty)} \left[\frac{\partial C}{\partial y}\right]_{y=0}$
$Sh\,Pe^{\frac{-1}{2}}$	dimensionless Sherwood number	$-\xi^{\frac{1}{2}} \left[1 + Pe_\zeta \ f'(\xi, 0)\right] \phi'(\xi, 0)$
T	temperature	K
T	dimensionless temperature	(–)
T_f	wall temperature	K
T_∞	ambient temperature	K
u, v	velocity components	$\mathrm{m/s}$
u_∞	free stream velocity	$\mathrm{m/s}$
x	axial coordinate	m
y	normal coordinate	m

Greek Symbols

α	thermal diffusivity	m^2/s
α_1	nonlinear density-temperature (NDT) parameter	$\frac{\beta_1(T_f-T_\infty)}{\beta_0}$
α_2	nonlinear density-concentration (NDC) parameter	$\frac{\beta_3(C_w-C_\infty)}{\beta_2}$
β_0, β_1	coefficients of thermal expansion of first and second orders	$(1/K, 1/K)$
β_2, β_3	coefficients of solutal expansion of first and the second order	$(m^3/kgmol, m^3/kgmol)$
η	similarity variable	(–)
λ	mixed convection parameter	$\frac{Ra}{Pe}$
Ω	inclination of angle	(–)
μ^*	fluid consistency of the power-law fluid	$kg/(ms)$
ν	kinematic viscosity	m^2/s
ρ	density of the fluid	kg/m^3
ψ	stream function	(–)
ξ	stream-wise coordinate	(–)

Subscripts

w	conditions at the wall	(–)
∞	conditions at the ambient medium	

Acknowledgements This work was supported by of Council of Scientific and Industrial Research (CSIR), New Delhi, India (Project No 25 (0246)/15 /EMR-II).

References

1. Shenoy A (1993) Darcy-Forchheimer natural, forced and mixed convection heat transfer in non-Newtonian power-law fluid saturated porous media. Transp Porous Media 11(3):219–241
2. Shenoy A (1994) Non-Newtonian fluid heat transfer in porous media. Adv Heat Transf 24:102–191
3. Gorla RSR, Kumari M (1999) Nonsimilar solutions for mixed convection in non-Newtonian fluids along a wedge with variable surface temperature in a porous medium. Int J Numerical Methods Heat Fluid Flow 9(5):601–611
4. Ibrahim F, Abdel Gaid S, Gorla RSR (2000) Non-Darcy mixed convection flow along a vertical plate embedded in a non-Newtonian fluid saturated porous medium with surface mass transfer. Int J Numerical Methods Heat Fluid Flow 10(4):397–408
5. Kumari M, Nath G (2004) Non-Darcy mixed convection in power-law fluids along a non-isothermal horizontal surface in a porous medium. Int J Eng Sci 42(3–4):353–369
6. Cheng CY (2008) Double-diffusive natural convection along a vertical wavy truncated cone in non-Newtonian fluid saturated porous media with thermal and mass stratification. Int Commun Heat Mass Transf 35(8):985–990
7. Kairi R, RamReddy C (2014) Solutal dispersion and viscous dissipation effects on non-Darcy free convection over a cone in power-law fluids. Heat Transf-Asian Res 43(5):476–488
8. Nield DA, Bejan A et al (2006) Convection in porous media, vol 3. Springer, Heidelberg
9. Murthy P (2000) Effect of double dispersion on mixed convection heat and mass transfer in non-Darcy porous medium. J Heat Transf 122(3):476–484
10. El Amin MF (2004) Double dispersion effects on natural convection heat and mass transfer in non-Darcy porous medium. Appl Math Comput 156(1):1–17

11. Kairi R, Murthy P (2010) Effect of double dispersion on mixed convection heat and mass transfer in a non-Newtonian fluid saturated non-Darcy porous medium. J Porous Media 13(8):749–757
12. RamReddy C (2013) Effect of double dispersion on convective flow over a cone. Int J Nonlinear Sci 15(4):309–321
13. Bouaziz A, Hanini S (2016) Double dispersion for double diffusive boundary layer in non-Darcy saturated porous medium filled by a nanofluid. J Mech 32(4):441–451
14. Barrow H, Sitharamarao T (1971) Effect of variation in volumetric expansion coefficient on free convection heat transfer. Br Chem Eng 16(8):704–709
15. Vajravelu K, Sastri K (1977) Fully developed laminar free convection flow between two parallel vertical walls-I. Int J Heat Mass Transf 20(6):655–660
16. Partha M (2010) Nonlinear convection in a non-Darcy porous medium. Appl Math Mech 31(5):565–574
17. Kameswaran P, Sibanda P, Partha M, Murthy P (2014) Thermophoretic and nonlinear convection in non-Darcy porous medium. J Heat Transf 136(4)
18. Munir AF, Tasawar H, Bashir A (2014) Peristaltic flow in an asymmetric channel with convective boundary conditions and Joule heating. J Central South Univ 21(4):1411–1416
19. Hayat T, Hussain M, Shehzad S, Alsaedi A (2016) Flow of a power-law nanofluid past a vertical stretching sheet with a convective boundary condition. J Appl Mech Tech Phys 57(1):173–179
20. RamReddy C, Naveen P (2019) Analysis of activation energy in quadratic convective flow of a micropolar fluid with chemical reaction and suction/injection effects. Multidisc Modeling Mater Struct 16(1):169–190
21. Murthy P, Singh P (1999) Heat and mass transfer by natural convection in a non-Darcy porous medium. Acta Mechanica 138(3–4):243–254
22. Chen HT et al (1988) Free convection flow of non-Newtonian fluids along a vertical plate embedded in a porous medium. J Heat Transf (Trans ASME (Am Soc Mech Eng) Ser C) (United States) 110(1)
23. Huang M, Huang J, Chou Y, Chen C (1989) Effects of Prandtl number on free convection heat transfer from a vertical plate to a non-Newtonian fluid. J Heat Transf (Trans ASME (Am Soc Mech Eng) Ser C) (United States) 111(1)
24. Chamkha AJ, Ahmed SE, Aloraier AS (2010) Melting and radiation effects on mixed convection from a vertical surface embedded in a non-Newtonian fluid saturated non-Darcy porous medium for aiding and opposing eternal flows. Int J Phys Sci 5(7):1212–1224
25. Prasad J, Hemalatha K, Prasad B (2014) Mixed convection flow from vertical plate embedded in non-Newtonian fluid saturated non-Darcy porous medium with thermal dispersion-radiation and melting effects. J Appl Fluid Mech 7(3):385–394
26. Sparrow E, Yu H (1971) Local non-similarity thermal boundary-layer solutions. J Heat Transf 93(4):328–334
27. Awad F, Sibanda P, Motsa SS, Makinde OD (2011) Convection from an inverted cone in a porous medium with cross-diffusion effects. Comput Math Appl 61(5):1431–1441
28. Khidir AA, Narayana M, Sibanda P, Murthy P (2015) Natural convection from a vertical plate immersed in a power-law fluid saturated non-Darcy porous medium with viscous dissipation and Soret effects. Afrika Matematika 26(7):1495–1518
29. RamReddy C, Naveen P (2019) Analysis of activation energy and thermal radiation on convective flow of a power-law fluid under convective heating and chemical reaction. Heat Transf-Asian Res 48(6):2122–2154
30. Canuto C, Hussaini MY, Quarteroni A, Thomas Jr A et al (2012) Spectral methods in fluid dynamics. Springer Science & Business Media
31. Chaoyang W, Chuanjing T, Xiaofen Z (1990) Mixed convection of non-Newtonian fluids from a vertical plate embedded in a porous medium. Acta Mechanica Sinica 6(3):214–220
32. Chen C (2004) Heat and mass transfer in MHD flow by natural convection from a permeable, inclined surface with variable wall temperature and concentration. Acta Mechanica 172(3):219–235

33. Aziz A (2009) A similarity solution for laminar thermal boundary layer over a flat plate with a convective surface boundary condition. Commun Nonlinear Sci Numerical Simul 14(4):1064–1068
34. Makinde O (2010) On MHD heat and mass transfer over a moving vertical plate with a convective surface boundary condition. Canadian J Chem Eng 88(6):983–990
35. Pal D, Chatterjee S (2013) Soret and dufour effects on MHD convective heat and mass transfer of a power-law fluid over an inclined plate with variable thermal conductivity in a porous medium. Appl Math Comput 219(14):7556–7574
36. Sui J, Zheng L, Zhang X, Chen G (2015) Mixed convection heat transfer in power-law fluids over a moving conveyor along an inclined plate. Int J Heat Mass Transf 85:1023–1033